COBEM 2021 26th International Congress of Mechanical Engineering
November 22-26, 2021, Virtual Congress, Brazil
ABCM Associação Brasileira de Engenharia e Ciências Mecânicas

COB-2021-2117
NUMERICAL SIMULATION OF TRANSPORT THROUGH POLYMER LAYER AND POROUS ARTERIAL WALL OF SIROLIMUS AND PACLITAXEL IN DRUG-ELUTING STENTS

H. Rosman
R. Lucena
N. Mangiavacchi
J. Pontes
Rio de Janeiro State University, Rio de Janeiro, RJ, Brazil
haroldo.rrj@gmail.com, rachel.lucena@gmail.com, norberto@uerj.br, jose.pontes@uerj.br

S. McGinty
Division of Biomedical Engineering, University of Glasgow, Glasgow, UK
sean.mcginty@glasgow.ac.uk

Abstract. *Drug-eluting stents are widely used but it is associated with the occurrence of restenosis and late stent thrombosis. Thus, the correct concentration of the eluted drug is very important to reduce the risk of both restenosis and thrombosis. This paper aims to analyze the drug elution from the polymer coating, transport, specific and non-specific binding in the artery wall for two different drugs, sirolimus and paclitaxel. The elution for two different release regimes, fast and slow, associated with two different polymer diffusion coefficients, was analyzed. In this paper a computational model is developed employing the Finite Element Method on an unstructured mesh. We consider the model of dissolution, transport and binding of the drug on an axisymmetric domain representing the polymer coating layer and the porous artery wall in the vicinity of a stent strut. We employ a nonlinear dissolution model for the dynamics of sirolimus or paclitaxel in the polymer coating, and a nonlinear saturable binding model that includes both specific and non-specific binding in the arterial wall as separate phases. The transport of the eluting drug in the artery wall is modeled considering an anisotropic diffusion tensor. The principal directions of the diffusion tensor are re-oriented in the vicinity of the stent to properly account for the compression and realignment of tissue fibers. Simulations performed with the developed computational model allow to fine-tune the polymer diffusion coefficient, and other geometric tunable parameters, in order to obey the required restraints for a safe drug-eluting stents utilization.*

Keywords: *drug-eluting stents, Darcy's law, convection-diffusion-reaction equations, anisotropic diffusion, Finite Element Method*

1. INTRODUCTION

Cardiovascular disease (CVD) is one of the main causes of death in the world, according to the World Health Organization (2021), reaching 17.9 million in 2019. Close to 40% of CVD deaths are due to coronary artery disease (CAD). The CAD is the result of obstruction of the coronary arteries - the blood vessels that supply the heart muscle, caused for example by smoking, high cholesterol, obesity, etc. One of the most popular treatments for CAD is to employ a stent, a are tiny expansible wire tube that is inserted in the obstructed coronary artery to maintain widen the lumen. However, bare-metal stents have shown the occurrence of restenosis, which is the obstruction of the artery due to arterial tissue regrowth. There are many works related to Drug-eluting stents (DES), which are typically coated with a polymer that slowly releases a drug that controls the arterial wall regrowth. Although DES are widely used, it is associated with cases of restenosis in less than 5% of cases and also the occurrence of late stent thrombosis in 1% of cases, despite being a more dangerous disease, as shown by Byrne *et al.* (2015). Thus, the correct concentration of the eluted drug is very important to reduce the risk of both restenosis and thrombosis, As shown by Bozsak *et al.* (2015), optimizing the period of drug release from DES and the initial drug concentration within the coating has a drastic effect on DES performance: this paper aims to analyse the application for two drugs, paclitaxel and sirolimus, in two different drug release regimes.

The safety and efficacy of DES are strongly influenced by the anisotropic transport of the antiproliferative/anti-inflammatory drugs in the arterial wall. Dissolution in the polymer coating and specific binding in the artery wall play an important role in the process. In this paper a computational model is developed employing the Finite Element Method (FEM) on an unstructured mesh to discretise the governing equations. We consider the model of dissolution, transport

and binding of the drug on an axisymmetric domain representing the polymer coating layer and the porous artery wall in the vicinity of a stent strut. We employ a nonlinear dissolution model for the dynamics of sirolimus or paclitaxel in the polymer coating, and a nonlinear saturable binding model that includes both specific and non-specific binding in the arterial wall as separate phases, as proposed by McGinty and Pontrelli (2016).

In a previous work Lucena *et al.* (2018) the diffusion tensor in the artery wall was considered orthotropic, with principal directions aligned with longitudinal (larger diffusion eigenvalue) and radial (smaller diffusion eigenvalue) directions, due to the orientation of tissue fibers in the artery wall, particularly plain muscle fibers in fine bundles, arranged in lamellae and disposed circularly around the vessel.

After that Frazzoli *et al.* (2020) modeled the transport of the eluting drug in the arterial wall considering an anisotropic diffusion tensor. The presence of the stent causes the compression and realignment of tissue fibers, such that they are parallel to the stent surface in its proximity. So, the principal directions of the diffusion tensor are re-oriented in the vicinity of the stent to properly account for this stent-artery interaction.

The flow is considered to be governed by Darcy flow. We consider the effect of the variation of the polymer properties, to show that the time evolution of the process can be efficiently controlled by the polymer diffusion coefficient.

This paper aims to analyze the drug elution from the polymer coating, transport, specific and non-specific binding in the artery wall for two different drugs, sirolimus and paclitaxel. The contribution of this work is to analyze the elution for two different release regimes, fast and slow, associated with two different polymer diffusion coefficients. Simulations performed with the developed computational model allow to fine-tune the polymer diffusion coefficient, and other geometric tunable parameters, in order to obey the required restraints for a safe DES utilization.

Since a full set of paclitaxel binding parameters are not readily available in the literature, for the purposes of this study we assume the binding parameters of paclitaxel match those of sirolimus.

2. THE MATHEMATICAL MODEL AND NUMERICAL METHOD

In this work we assume a geometric symmetry about a reference axis, and therefore we employ an axisymmetric formulation. Figure 1(a) shows the model geometry where z direction is the axis of symmetry and r is the radial direction. The region Ω_1 represents the polymer layer and Ω_2 represents the arterial wall. Using the mesh generator tool Gmsh we create a two-dimensional unstructured triangular mesh, as shown in Fig. 1(b), which is used in the simulations.

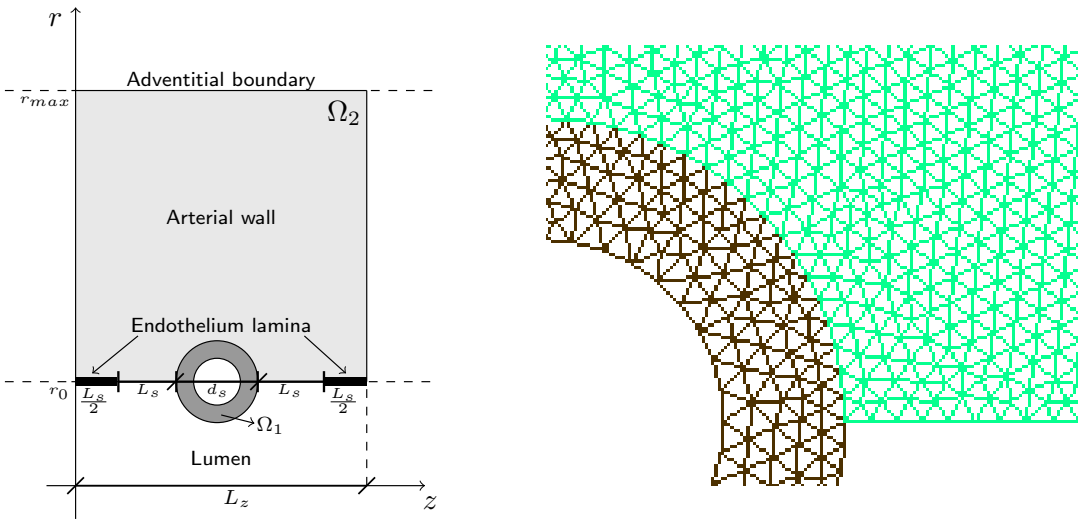

(a) (b)

Figure 1. (a) Model 2D axisymmetric geometry. Note that the endothelium is assumed to be denuded in the vicinity of the stent strut. (b) Detail of the computational domain and unstructured triangular mesh employed in the simulations. Black: polymer layer Ω_1. Green: arterial wall Ω_2.

We adopt the modeling framework of Bozsak *et al.* (2014) and McGinty and Pontrelli (2016). The arterial wall and the polymer layer are considered as porous media, and flow within these layers is assumed to be governed by Darcy's law ((Bear, 2013)),

$$\mathbf{u} = -\frac{P_{D_i}}{\mu}\nabla p \tag{1}$$

and to be incompressible, $\nabla \cdot \mathbf{u} = 0$, thus,

$$\nabla \cdot \left(-\frac{P_{D_i}}{\mu} \nabla p \right) = 0, \tag{2}$$

where $\mathbf{u} = (u, v)$ is the velocity field with radial and axial components, respectively, p is the pressure in the arterial wall, P_{Di} is the Darcy permeability of the media and μ is the fluid viscosity.

As proposed by McGinty and Pontrelli (2016), the drug dynamics in the coating is modeled in terms of b_0 (solid) and c_0 (dissolved) concentrations by the equations:

$$\frac{\partial b_0}{\partial t} = -\beta_0 b_0^{2/3}(S_0 - c_0) \tag{3}$$

$$\frac{\partial c_0}{\partial t} + \mathbf{u}_s \cdot \nabla c_0 = \nabla \cdot (\mathcal{D}_0 \nabla c_0) + \beta_0 b_0^{2/3}(S_0 - c_0), \tag{4}$$

where $\mathbf{u}_s = \mathbf{u}/\phi_i$ is the seepage velocity, and ϕ_i is the effective porosity of the media, $\mathcal{D}_0$ is the effective scalar diffusion coefficient of the solute, β_0 the dissolution rate and S_0 is the solubility limit.

Drug elution in the arterial wall is governed by the convection-diffusion-reaction equations:

$$\frac{\partial c_1}{\partial t} + \mathbf{u}_s \cdot \nabla c_1 = \nabla \cdot (\mathcal{D}_1 \nabla c_1) - k_1^f c_1 (b_1^{max} - b_1) + k_1^r b_1 - k_2^f c_1 (b_2^{max} - b_2) + k_2^r b_2 \tag{5}$$

$$\frac{\partial b_1}{\partial t} = k_1^f c_1 (b_1^{max} - b_1) - k_1^r b_1 \tag{6}$$

$$\frac{\partial b_2}{\partial t} = k_2^f c_1 (b_2^{max} - b_2) - k_2^r b_2 \tag{7}$$

where c_1 is the concentration of a drug transported in the arterial wall, b_1 and b_2 denote non-specifically and specifically bound drug, respectively, The effectiveness of the drug delivery depends on the specifically bound concentration. The k_i^f, k_i^r, b_i^{max} are constant parameters related to the binding kinetics, and $\mathcal{D}_1$ is the diffusion coefficient, given by an anisotropic tensor,

$$\mathcal{D}_1 = \begin{bmatrix} \mathcal{D}_{1rr} & \mathcal{D}_{1rz} \\ \mathcal{D}_{1zr} & \mathcal{D}_{1zz} \end{bmatrix}, \tag{8}$$

with r the radial direction and z the axial direction.

The tensor $\mathcal{D}_1$ is constructed from the principal directions α_i and the principal values λ_i, as: $\mathcal{D}_1 = P\Lambda P^{-1}$ where Λ is the diagonal matrix of the principal values, and P is the block matrix of column vectors α_i, given by $P = (\alpha_1 \alpha_2)$. The direction α_1 is perpendicular to the direction of the fibers of the arterial tissue and therefore it is associated to a smaller diffusion principal value λ_1, while the direction α_2 is tangent to the direction of the arterial fibers, hence associated to a large diffusion principal value λ_2. Values of λ_1 and λ_2 are taken from the radial and axial diffusion coefficients reported in the literature (Lucena *et al.* (2018)). To obtain an approximation of the direction perpendicular to the fibers (α_1) we employ the gradient of a marker function d

$$\alpha_1 = \nabla d \qquad \text{and} \qquad \nabla^2 d = 0, \tag{9}$$

where d is computed for every mesh point as the solution of the above equation. Subsequently, the direction α_2 is constructed employing orthogonality. Figure 2 shows a schematic of the principal directions, α_1 and α_2, close to the stent.

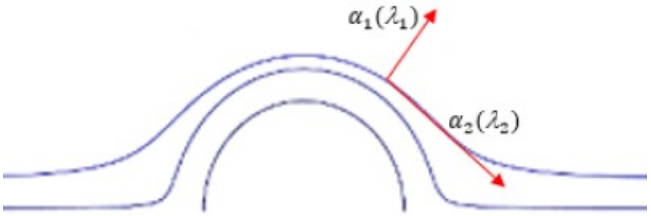

Figure 2. The schematic of the principal directions, α_1 and α_2, close to stent.

The permeability in the polymer coating, P_{D0}, is considered to be very small, but finite. The endothelium lamina, where present, is modeled as a no-flow boundary. The boundary conditions for drug concentration in the denuded endothelium is $c_1 = 0$, between polymer and lumen, i.e., on interface Γ_1 is $c_0 = 0$, (see Fig. 1,(a)), and in the interior surface of Ω_1, we impose zero flux (see Fig. 1,(a)). We assume periodic conditions at the side boundaries.

The mass flux is established across the interface and the drug starts to be transferred to the adjacent release medium. The instantaneous flux is given by:

$$\varphi_i(t) = \int_{\Gamma_i} \mathbf{n} \cdot \mathcal{D}_0 \nabla c_0(t) d\Gamma, \quad \text{with} \quad i = 1, 2, \tag{10}$$

where $i = 1$ refers to the lumen interface, $i = 2$ refers to the arterial wall, $\mathbf{n}$ is the surface normal, and $d\Gamma = 2\pi r d\theta$. The mass flux (integral) is given by:

$$\Phi_i = \int_0^t \varphi_i(t) dt, \tag{11}$$

where t is the time.

The governing equations in 2D axisymmetric coordinates are solved on an unstructured triangular mesh, using linear base functions and the Galerkin Finite Element Method (see Lucena *et al.*, 2018). The convective terms are discretized using a semi-Lagrangian approach. A semi-implicit fractional step method is employed for the convection–diffusion–reaction equations. The dimensional parameters employed in the simulations are shown in Tab. 1. All the simulations were performed with an in-house code, which was written in Octave language.

Table 1. Dimensional parameters used in the simulations. Values of $r_0, r_{max} - r_0, d_s, L_s, L_p, L_z, p_{wall}, \mu, D_0, P_{D1}, \phi_1, D_{1r}, D_{1z}$ were obtained from Bozsak *et al.* (2014). Values of $\beta_0, B_0, S_0, k_1^f, k_1^r, b_1^{max}, k_2^f, k_2^r, b_2^{max}$ were obtained from McGinty and Pontrelli (2016).

Parameter		**Simulated value**
r_0	Lumen radius	1.5×10^{-3}m
$r_{max} - r_0$	Arterial wall thickness	5.0×10^{-4}m
d_s	Stent strut diameter	2.5×10^{-4}m
L_s	Denuded endothelium	1.5×10^{-4}m
L_p	Polymer thickness	5.0×10^{-5}m
L_z	Domain length	7.0×10^{-4}m
p_{wall}	Lumen overpressure	9.31×10^3 Pa
μ	Fluid viscosity	7.2×10^{-4} Pa.s
dt	Simulation time step	100s
t_{end}	Time of simulation	20 and 200 days
	Polymer layer	
P_{D0}	Permeability	2.78×10^{-21}m^2
ϕ_0	Porosity	0.29
β_0	Dissolution rate	1.0×10^{-4}(mol.m^{-3})$^{-2/3}$.s^{-1}
B_0	Initial drug eluting	100 mol.m^{-3}
S_0	Drug solubility	$B_0/10$ mol.m^{-3}
$\mathcal{D}_0$	Fast diffusion coefficient	1.0×10^{-14}m^2.s^{-1}
$\mathcal{D}_0$	Slow diffusion coefficient	1.0×10^{-15}m^2.s^{-1}
	Arterial wall	
P_{D1}	Permeability	2.0×10^{-18}m^2
ϕ_1	Porosity	0.29
k_1^f	Association rate constant of non-specifically bound	2 (mol.m^{-3}.s)$^{-1}$
k_1^r	Dissociation rate constant of non-specifically bound	5.2×10^{-3} s^{-1}
b_1^{max}	Local density of non-specifically binding sites	3.63×10^{-1} mol.m^{-3}
k_2^f	Association rate constant of specifically bound	800 (mol.m^{-3}.s)$^{-1}$
k_2^r	Dissociation rate constant of specifically bound	$1.6 \times 10^{-4} s^{-1}$
b_2^{max}	Local density of specifically binding sites	3.3×10^{-3} mol.m^{-3}
	Sirolimus	
$\mathcal{D}_{1r} = \lambda_1$	Radial diffusion coefficient	7×10^{-12}m^2.s^{-1}
$\mathcal{D}_{1z} = \lambda_2$	Axial diffusion coefficient	4×10^{-11}m^2.s^{-1}
	Paclitaxel	
$\mathcal{D}_{1r} = \lambda_1$	Radial diffusion coefficient	2×10^{-12}m^2.s^{-1}
$\mathcal{D}_{1z} = \lambda_2$	Axial diffusion coefficient	5×10^{-11}m^2.s^{-1}

3. COMPUTATIONAL RESULTS AND DISCUSSION

Simulations were performed considering two different polymer layer diffusion coefficients (fast and slow), for the two drugs, sirolimus and paclitaxel, and using data summarized in Tab. 1. The pressure and velocity distributions are assumed constant along the simulation of both drugs transport (not shown).

A mesh convergence study was performed in Frazzoli (2020) and showed a sub-quadratic precision. The mesh employed in the current simulations is comprised of 7,016 triangular elements and 3,489 nodes, resulting on an estimated relative mass error of 0.5%.

In the beginning of the simulation all the drug is in solid form, contained in the polymer layer, with concentration B_0, and null concentration elsewhere. For both drugs, the solid gradually dissolves in the polymer layer and diffuses to the porous artery wall.

Results are shown as color maps of concentration at representative times, and time plots of drug flux, in Figs. 3 to 12.

3.1 Fast regime release

For the concentration, c_1, Fig. 3(a)-(b) shows that for 2 days c_1 starts to leave the stent and penetrate the arterial wall for sirolimus and paclitaxel, being a little faster for the last one. In 15 days, paclitaxel reaches almost the entire arterial wall and sirolimus behavior is similar but somewhat slower (see Fig. 3(c)-(d)). For both times, paclitaxel reaches higher concentrations over most of the arterial wall region.

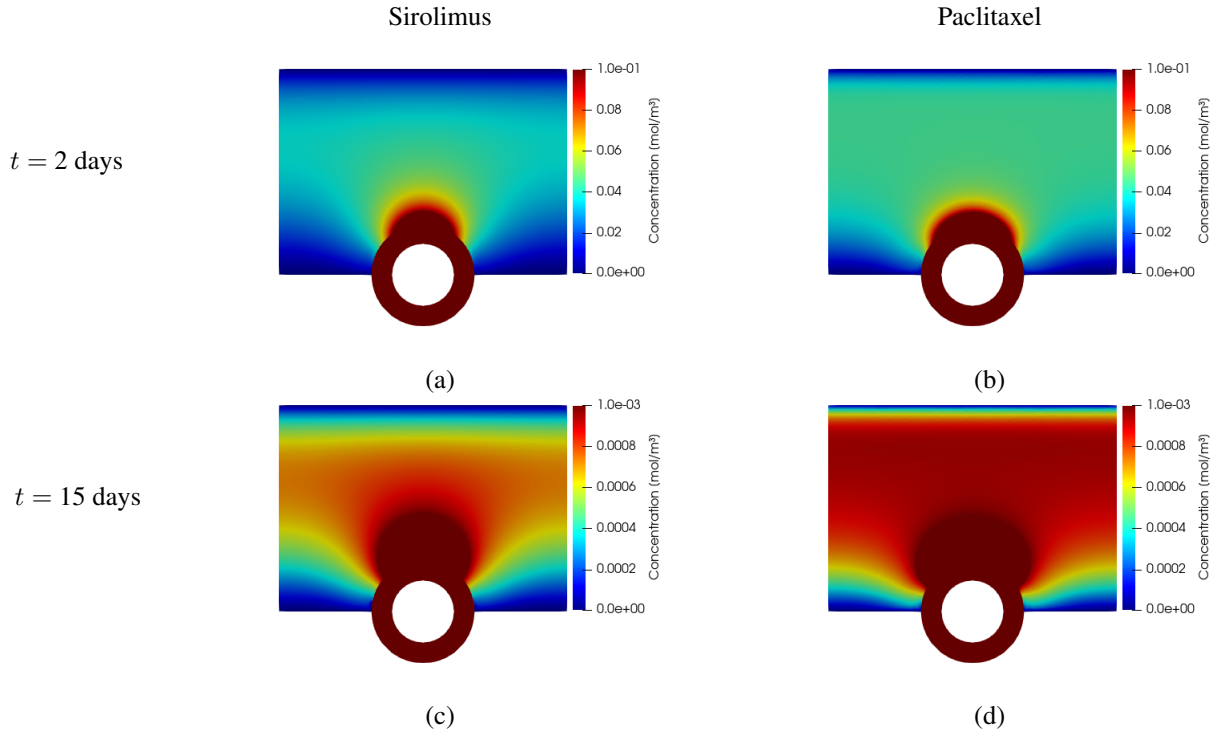

Figure 3. Concentration c_1 in the fast regime for sirolimus, (a) and (c), and paclitaxel, (b) and (d), at the second day, (a) and (b), and at the fifteenth day, (c) and (d).

Figure 4(a)-(b), shows that in two days the non-specifically bound drug concentration, b_1, quickly reaches the saturation level b_1^{max} in the arterial wall, and in the polymer layer we have the solid bound drug concentration, b_0, still almost saturated for both drugs. At $t = 15$ days the sirolimus deflates at the top of the arterial wall and next to endothelium lamina and the stent, while for the paclitaxel b_1 remains high on a wider region in the middle of the arterial wall and the top of stent, and in the polymer layer $b_0 \approx 0$, as can be seen in Fig. 4(c)-(d).

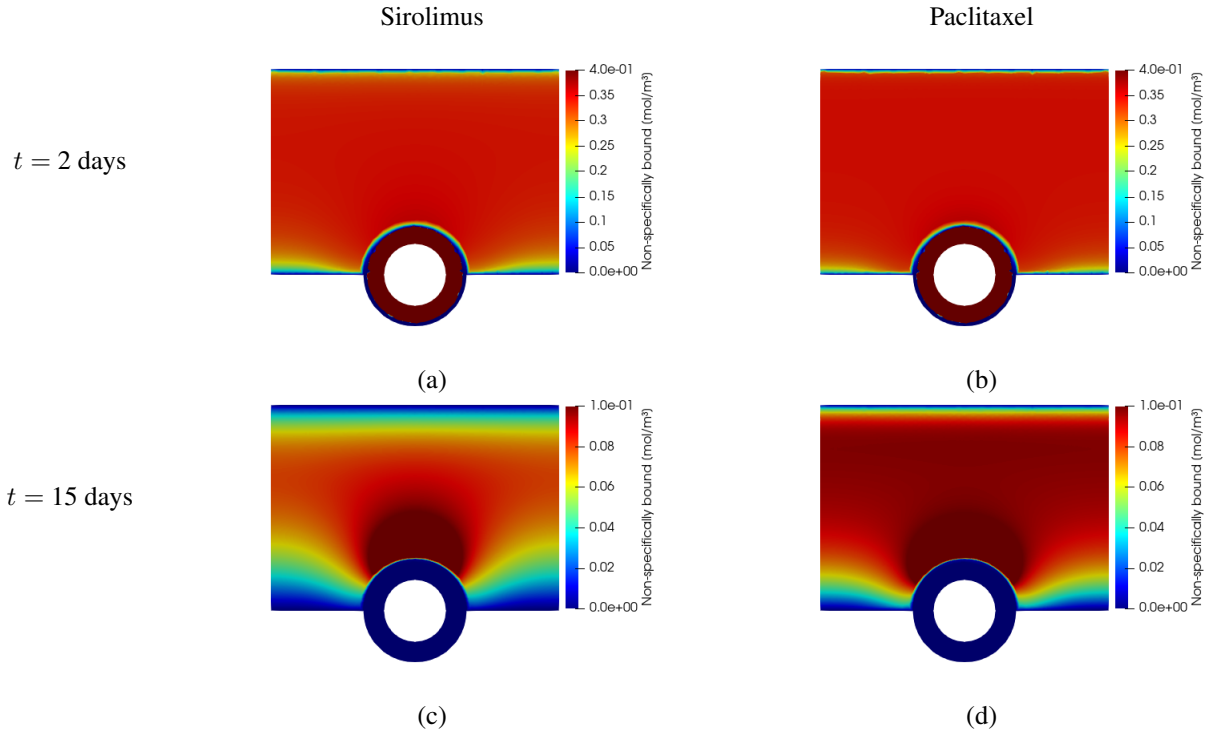

Figure 4. Solid bound drug, b_0, at the polymer layer and non-specifically bound drug, b_1 at the arterial wall in the fast regime for sirolimus, (a) and (c), and paclitaxel, (b) and (d), at the second day, (a) and (b), and at the fifteenth day, (c) and (d).

Similarly for b_1, Fig. 5 shows that the specifically bound drug b_2 gets the maximum value in 2 days over practically all the arterial wall for both drugs, and in 15 days the wall is still completely saturated.

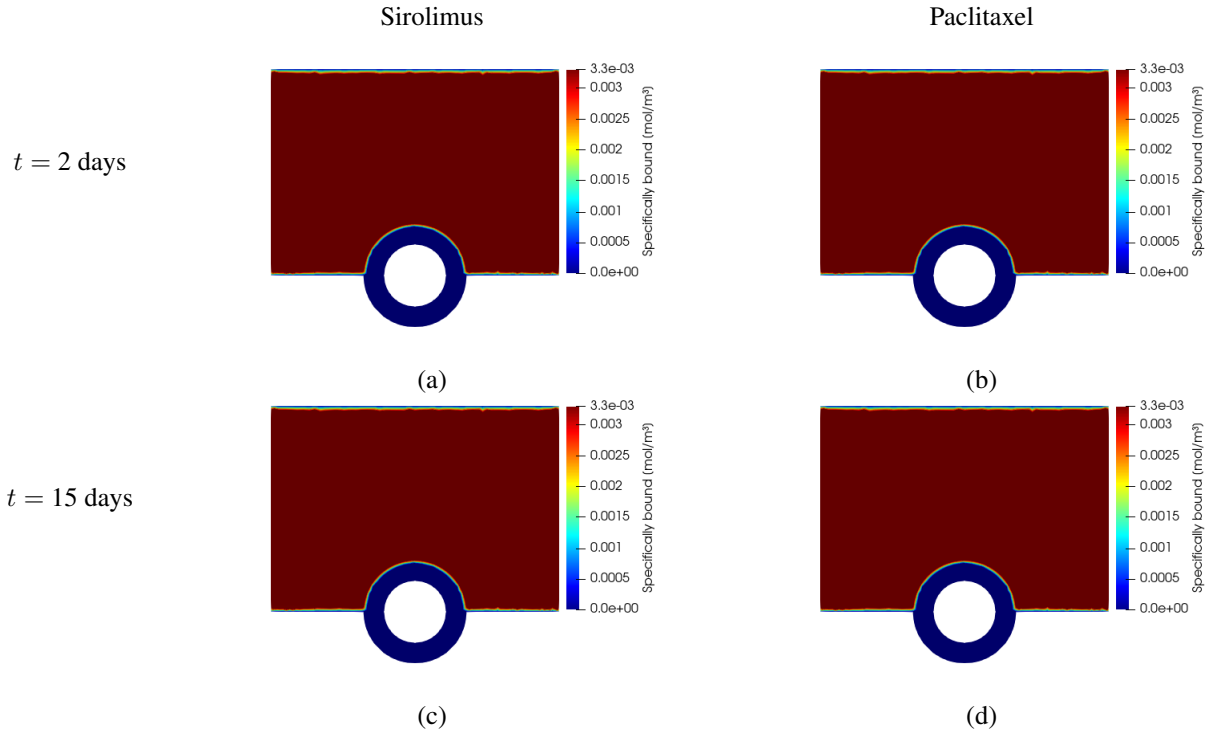

Figure 5. Specifically bound drug b_2 in the fast regime for sirolimus, (a) and (c), and paclitaxel, (b) and (d), at the second day, (a) and (b), and at the fifteenth day, (c) and (d).

The average free concentration, c_1, and the average solid bound concentration, b_0, for sirolimus and paclitaxel have very similar behavior as can observed in Fig. 6(a)-(b). For the non-specifically bound, b_1, the drugs have similar behaviors, although paclitaxel remains slightly larger than sirolimus. Finally, for specifically bound, b_2, for both drugs stay fully

saturated up to day 17, when they start to drop but the sirolimus drops with a bigger gradient, as we can see in Fig. 6(c)-(d).

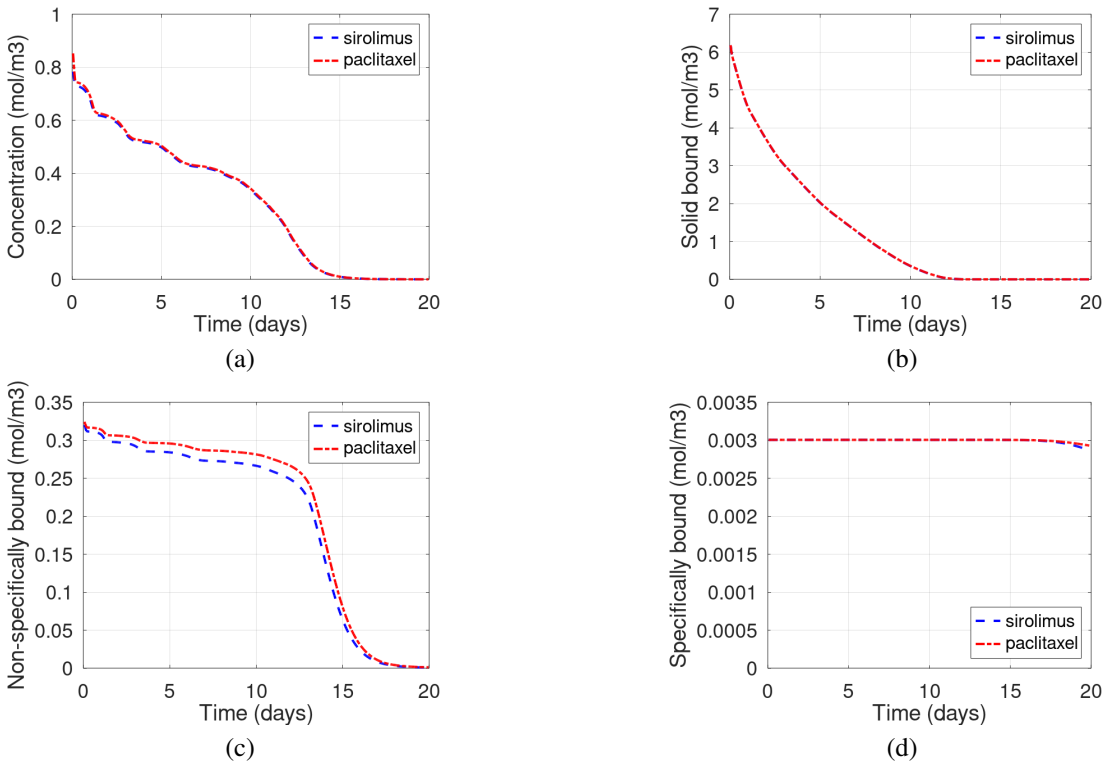

Figure 6. Comparison of average concentrations for the fast regime release. (a) Free concentration, (b) Solid bound, (c) Non-specifically bound, (d) Specifically bound.

Figure 7(a)-(b) shows the instantaneous (Eq. 10) and integral (Eq. 11) mass flux for paclitaxel and sirolimus though the arterial wall and lumen. We can observe that the instantaneous mass flux starts dropping for paclitaxel in the lumen and arterial wall. However, we can see a difference for the sirolimus behaviour in the lumen, it increases for a short time then it quickly drops with a bigger slope than paclitaxel. After the third day they follow approximately the same curve going to zero around the day 15, and this behavior is similar to both interfaces. The mass flux has a curve with a similar gradient for arterial wall and lumen. However, for both drugs the mass flux is bigger to the arterial wall than to the lumen.

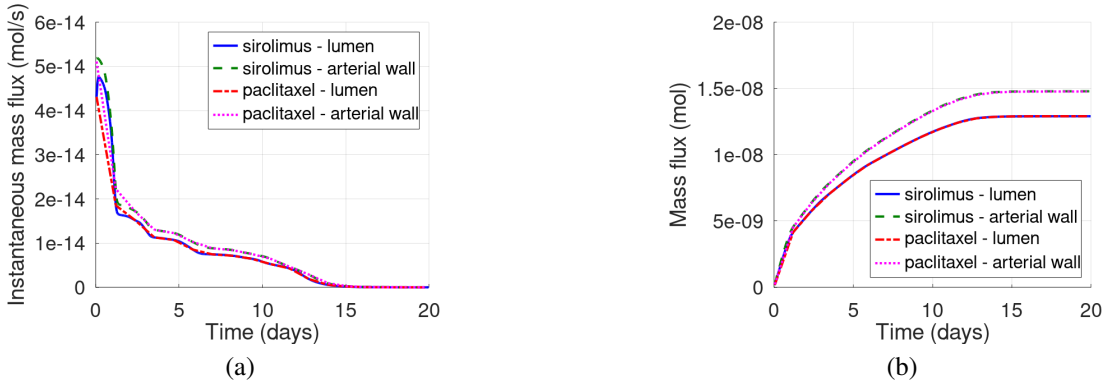

Figure 7. Comparison of the (a) instantaneous mass flux and (b) mass flux in the arterial wall and lumen for fast regime release.

3.2 Slow regime release

Figure 8(a)-(b) shows that, for slow regime release, after 20 days the concentration, c_1, has the similar behavior for sirolimus and paclitaxel as the fast regime at $t = 2$ days. In Fig. 8(c)-(d) we can see that at the day 200 both values of concentration are low, but the c_1 for paclitaxel is higher than for sirolimus over a large area.

For both drugs, at $t = 20$ days, there is a large area in the polymer layer with high solid bound drug concentration b_0, but at $t = 200$ days, the solid has completely dissolved, as we can see at the Fig. 9. The non-specifically bound drug, b_1,

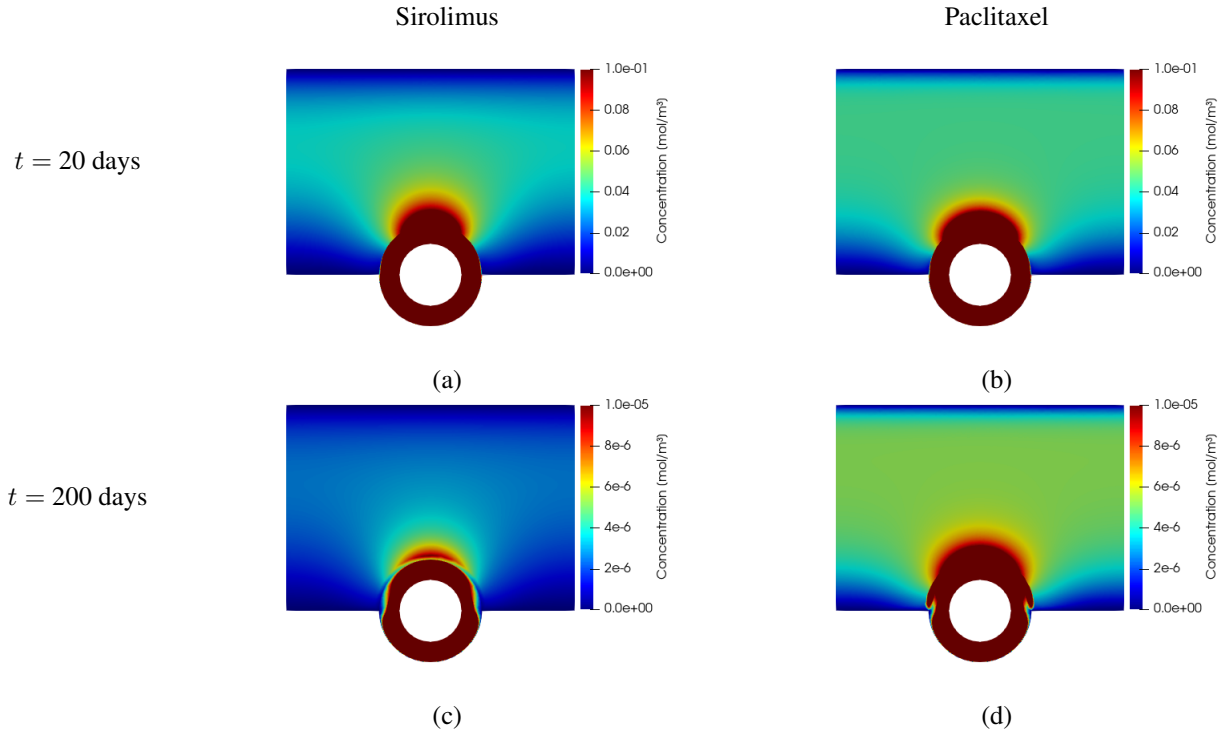

Figure 8. Concentration c_1 in the slow regime for sirolimus, (a) and (c), and paclitaxel, (b) and (d), at the day 20, (a) and (b), and at day 200, (c) and (d).

quickly reaches the saturation level b_1^{max} in the arterial wall for both drugs, similarly to the fast regime at two days. And at $t = 200$ days, the saturation level is low but for paclitaxel its still higher than sirolimus.

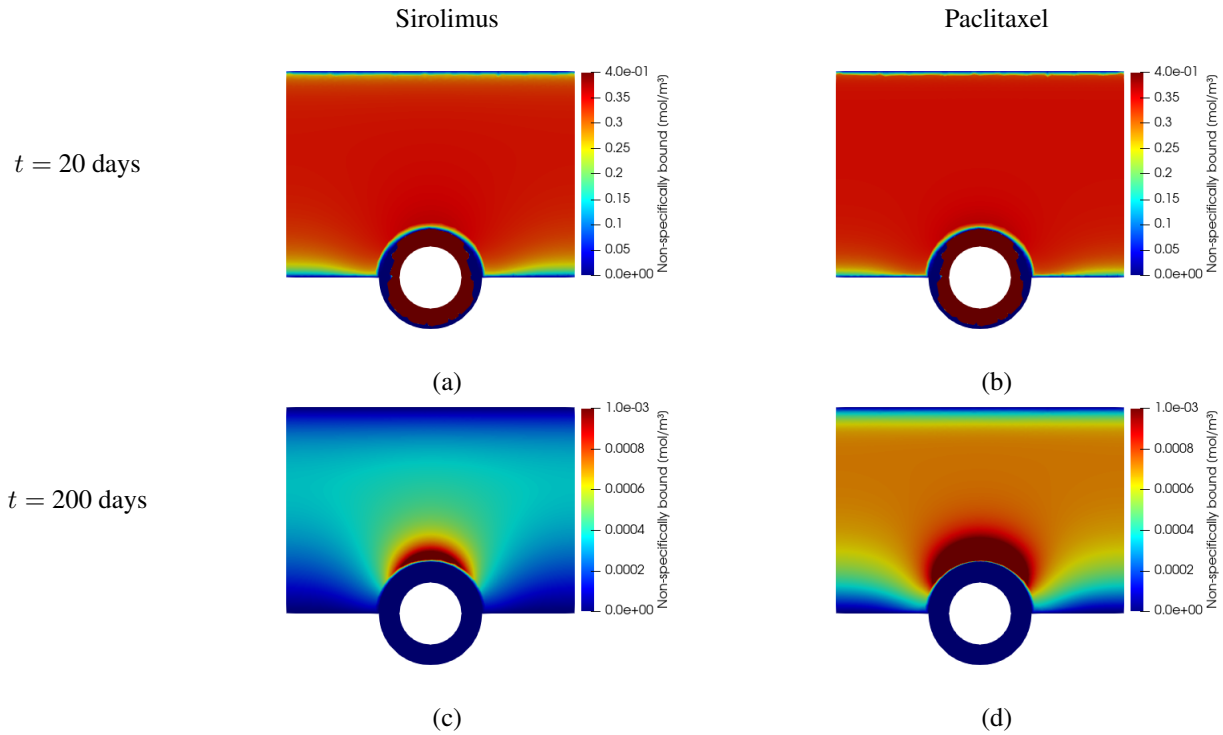

Figure 9. Solid bound drug, b_0, at the polymer layer and non-specifically bound drug, b_1 at the arterial wall in the slow regime for sirolimus, (a) and (c), and paclitaxel, (b) and (d), at the day 20, (a) and (b), and at day 200, (c) and (d).

The specifically bound drug, b_2, also gets the maximum value in 2 days over practically all the arterial wall for both drugs as for the fast regime as we can see at the Fig. 10(a)-(b). And in the day 200 the Fig. 10(c)-(d) shows that the value of b_2 only decreases next to the endothelium lamina for both drugs but its easier to see for the sirolimus.

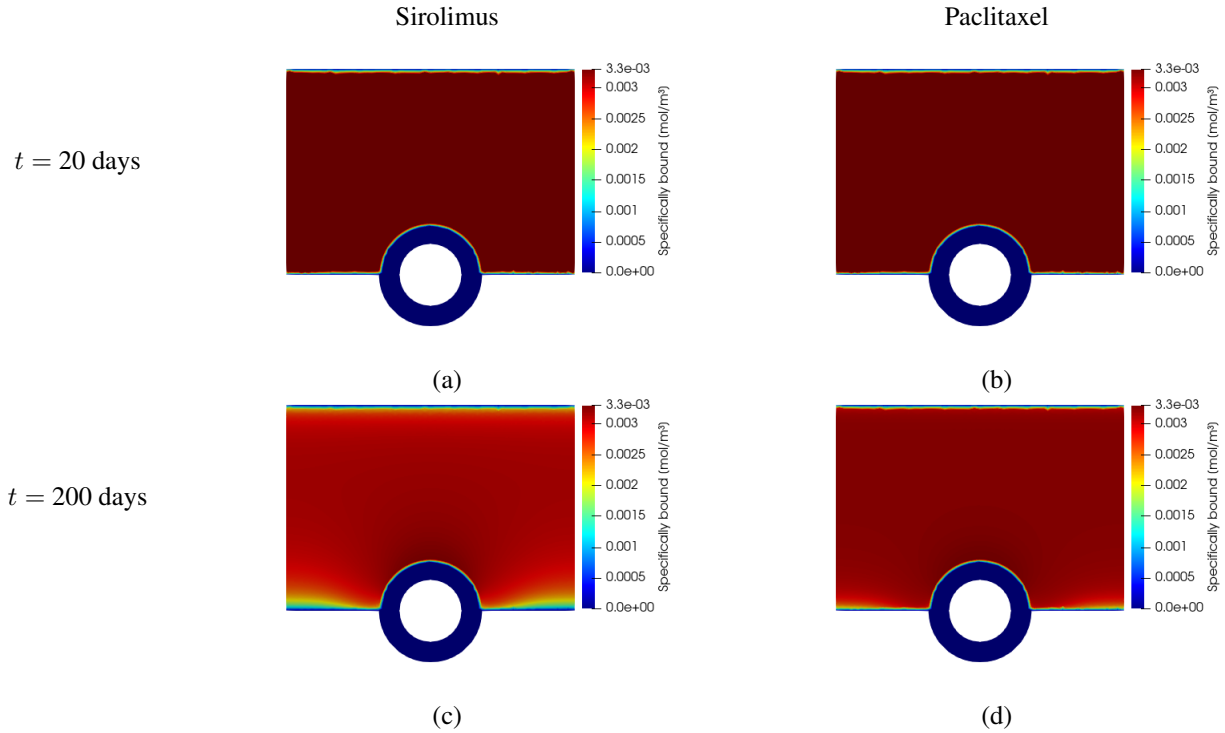

Figure 10. Specifically bound drug, b_2 in the slow regime for sirolimus, (a) and (c), and paclitaxel, (b) and (d), at the day 20, (a) and (b), and at day 200, (c) and (d).

Figure 11 shows that the difference between the drugs have the same behavior for the slow regime as the fast one, with some difference curve for c_1 and b_1.

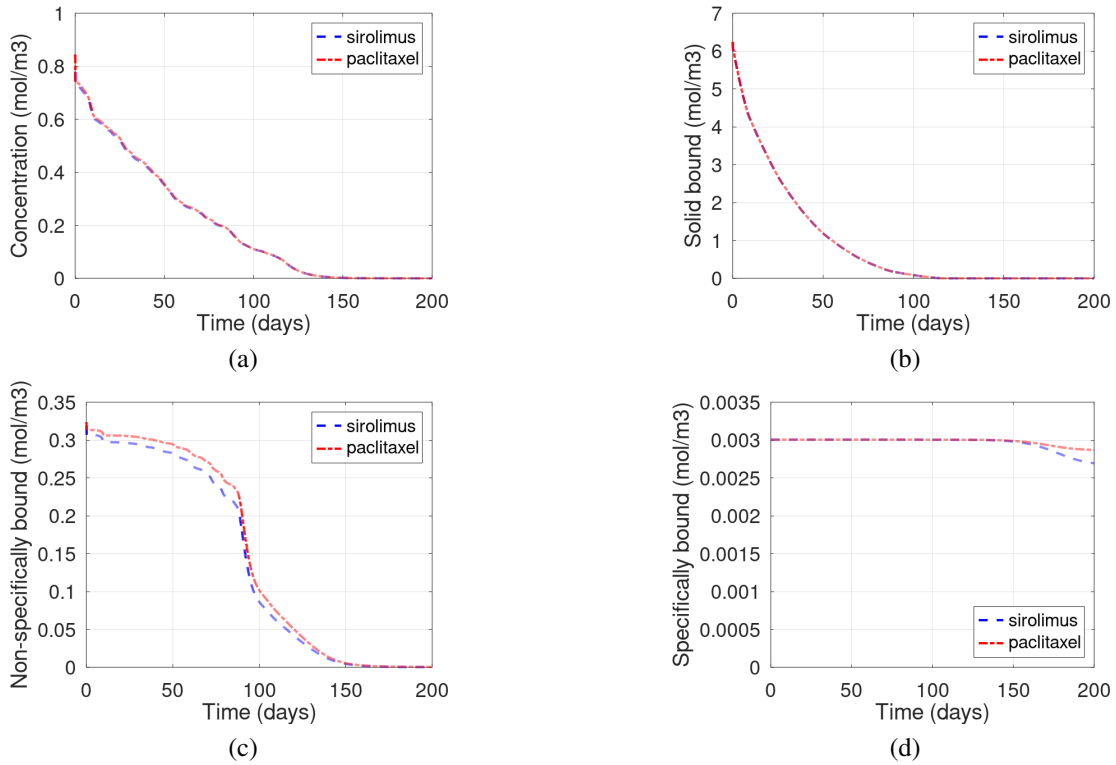

Figure 11. Comparison of concentrations for slow regime. (a) Concentration, (b) Solid bound, (c) Non-specifically bound, (d) Specifically bound.

For the slow regime, the difference between the curves for the two drugs is very small, as we can see at Fig.12(a)-(b). Figure 12(b) shows that the mass flux at the arterial wall increases faster than at the lumen, and for the instantaneous mass

flux, the Fig. 12(a) shows that in the arterial wall the flux drops to zero before than in the lumen.

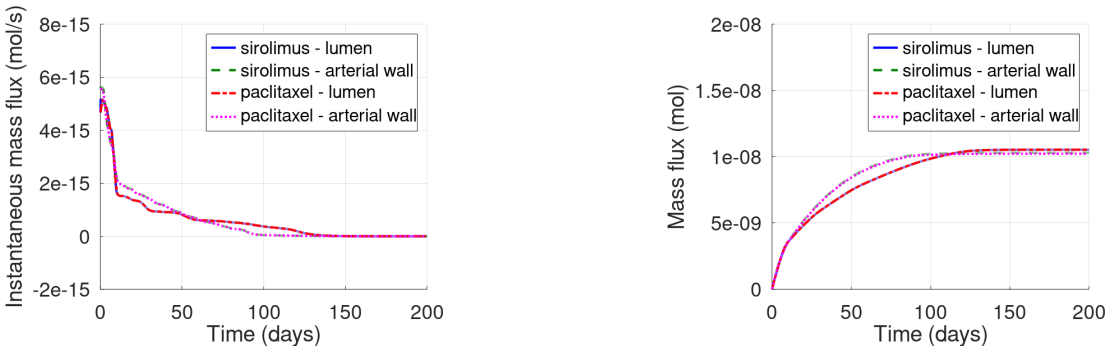

(a) (b)

Figure 12. Comparison of the (a) instantaneous and (b) integral mass flux in the arterial wall and lumen for slow regime.

4. CONCLUSIONS

Paclitaxel and sirolimus have a similar dissolution and diffusion behaviors. However, paclitaxel invades a larger portion of the arterial wall than sirolimus for both fast and slow polymer diffusion regimes, although the radial diffusion coefficient on the arterial wall of sirolimus is larger. The more uniform distributions of free and bound paclitaxel can be explained by the more anisotropic diffusion, with larger axial direction diffusion of paclitaxel compared with sirolimus.

Regarding the free concentration c_1 and the solid bound concentration b_0, sirolimus and paclitaxel have similar curves for both regimes. The same occurs for both specific and non-specific bound concentrations, but paclitaxel remains saturated for slightly longer times than sirolimus. The two drugs have almost the same behavior for both fast and slow regimes regarding the mass flow and the instantaneous mass flow, since these are mostly controlled by the dissolution rate.

For the purposes of this study we assumed that the binding parameters of paclitaxel match those of sirolimus. This is a limitations that will be addressed in future work.

5. ACKNOWLEDGEMENTS

The authors would like to acknowledge financial support from FAPERJ, CAPES, CNPq, and the University of Glasgow EPSRC GCF ISF fund.

6. REFERENCES

Bear, J., 2013. *Dynamics of fluids in porous media*. Courier Corporation.

Bozsak, F., Chomaz, J. and Barakat, A., 2014. "Modelling the transport drugs of eluted from stents: physical phenomena driving drug distribution in the arterial wall". *Biomech Model Mechanobiol*, Vol. 13, pp. 327–347.

Bozsak, F., Gonzalez-Rodriguez, D., Sternberger, Z., Belitz, P., Bewley, T., Chomaz, J.M. and Barakat, A.I., 2015. "Optimization of drug delivery by drug-eluting stents". *PLOS ONE*.

Byrne, R.A., Joner, M. and Kastrati, A., 2015. "Stent thrombosis and restenosis: what have we learned and where are we going? The Andreas Grüntzig Lecture ESC 2014". *European Heart Journal*.

Frazzoli, F., Rosman, H., Lucena, R., Mangiavacchi, N., Pontes, J., Anjos, G. and McGinty, S., 2020. "Improved anisotropic transport through polymer layer and porous arterial wall with binding in drug-eluting stents". In *18th Brazilian Congress of Thermal Sciences and Engineering*.

Frazzoli, F.A.S., 2020. *Anisotropic transport through polymer layer and porous arterial wall with binding in drug-eluting stents using the FEM*. Master's thesis, Rio de Janeiro State University.

Lucena, R., Mangiavacchi, N., Pontes, J., Anjos, G. and McGinty, S., 2018. "On the transport through polymer layer and porous arterial wall in drug-eluting stents". *Journal of the Brazilian Society of Mechanical Sciences and Engineering*, Vol. 40, No. 572.

McGinty, S. and Pontrelli, G., 2016. "On the role of specific drug binding in modelling arterial eluting stents". *J Math Chem*, Vol. 54, pp. 967–976.

World Health Organization, 2021. *World health statistics 2021: monitoring health for the SDGs, sustainable development goals*. World Health Organization.

7. RESPONSIBILITY NOTICE

The authors are the only responsible for the printed material included in this paper.